

Published in final edited form as:

Circulation. 2009 September 15; 120(11 Suppl): S22–S30. doi:10.1161/CIRCULATIONAHA.108.842724.

Effect of Hypercholesterolemia on Myocardial Necrosis and Apoptosis in the Setting of Ischemia-Reperfusion

Robert M. Osipov, MD¹, Cesario Bianchi, MD, PhD¹, Jun Feng, MD, PhD¹, Richard T. Clements, PhD¹, Yuhong Liu, MD¹, Michael P. Robich, MD¹, Hilary P. Glazer¹, Neel R. Sodha, MD², and Frank W. Sellke, MD FAHA, FACS^{1,3}

¹Division of Cardiothoracic Surgery, Beth Israel Deaconess Medical Center. Harvard Medical School. Boston, MA

²Department of Surgery, Beth Israel Deaconess Medical Center. Harvard Medical School. Boston, MA

³Alpert Medical School of Brown University, Providence, RA

Abstract

Background—Hypercholesterolemia is prevalent in patients who experience myocardial ischemia-reperfusion injury (IR). We investigate the impact of dietary induced hypercholesterolemia on the myocardium in the setting of acute IR.

Methods and Results—In normocholesterolemic (NC, n=7) and hypercholesterolemic (HC, n=7) Yucatan male pigs, the left anterior descending coronary artery was occluded for 60 min, followed by reperfusion for 120 min. Hemodynamic values were recorded and TTC staining was used to assess necrosis. Oxidative stress was measured. Specific cell death and survival signaling pathways were assessed by Western blot and TUNEL staining. Infarct size was 45% greater in HC vs. NC (42% vs. 61%, p<.05), whereas the area at risk (AAR) was similar in both groups (p=0.61). While global LV function (+dP/dt, p<.05) was higher during entire period of IR in HC vs. NC, regional function deteriorated more following reperfusion in HC (p<.05). Ischemia increased indices of myocardial oxidative stress such as protein oxidation (p<.05), lipid peroxidation (p<.05), and nitrotyrosylation in HC vs. NC, as well as the expression of phospho-eNOS (p<.05). The expression of myeloperoxidase, p38 MAPK, and phospho-p38 MAPK was higher in HC vs. NC (all p<.05). Ischemia caused higher expression of the pro-apoptotic protein PARP (p<.05), and lower expression of the pro-survival proteins Bcl2 (p<.05), phospho-Akt, (p<.05), and phospho-PKCε (p<.05) in the HC vs. NC. TUNEL positive cell count was 3.8 fold (p<.05) higher in the AAR of HC vs. NC.

Conclusions—This study demonstrates that experimental hypercholesterolemia is associated with increased myocardial oxidative stress and inflammation, attenuation of cell survival pathways and induction of apoptosis in the ischemic territory, which together may account for the expansion of myocardial necrosis in the setting of acute IR.

Keywords

apoptosis; hypercholesterolemia; ischemia; myocardial infarction; risk factors

Author for correspondence: Frank W. Sellke, MD, Beth Israel Deaconess Medical Center. 330 Brookline Ave. DANA 801, Boston, MA 02215, Phone: 401 444 2380, Fax 617 975 5588 617 632 8387, fsellke@caregroup.harvard.edu.

Disclosures

Dr. Frank W. Sellke has research support from Ikaria (Clinton, NJ) and Orthologic (Tempe, AZ), and he is a consultant for Novo Nordisk (Princeton, NJ) and Cubist Pharmaceuticals (Lexington, MA).

Introduction

Coronary artery disease (CAD) and acute myocardial infarction (AMI) are the largest cause of death in the World today. Prompt reperfusion via angioplasty, thrombolytic therapy, or coronary artery bypass surgery to salvage the ischemic myocardium is considered the optimal management for AMI ¹.

In recent years many studies have shown that hypercholesterolemia is not only detrimental for CAD progression but is also a risk factor for higher mortality and poor left ventricular systolic function in patients following AMI ^{2,3}. This suggests that hypercholesterolemia may adversely influence the evolution of AMI even after patency of an occluded coronary artery is successfully reestablished. However, the mechanisms responsible for enhanced cardiomyocyte injury following ischemia-reperfusion (IR) in patients with hypercholesterolemia are poorly understood.

To date, myocardial IR injury studies conducted in hypercholesterolemic animals (rabbits and rodents) have yielded varied and controversial findings. While some researchers reported that diet-induced hypercholesterolemia enhances myocardial injury by increasing oxidative stress ⁴, upregulation of inflammation ⁵, inhibition of nitric oxide synthesis ⁶, vascular obstruction ⁷, and increased cardiomyocyte apoptosis ⁸, others have found no additional harm after reperfusion injury ^{8,9}, or have shown that hypercholesterolemia improves myocardial function and may even be cardioprotective ¹⁰. In past decades the effects of hypercholesterolemia in a porcine model of acute myocardial IR was addressed in a single study which examined the impact of preconditioning and postconditioning on the myocardium ¹¹. In addition, most clinical studies are confounded by multiple cardiovascular risk factors other than hypercholesterolemia. In light of the clinical implications, these controversies deserve further investigation. In this study, we investigated the effects of hypercholesterolemia alone on the non-ischemic and ischemic myocardium in a porcine model of acute IR.

Materials & Methods

Animals

Intact Yucatan male mini-swine (20 weeks old) were divided into two groups: normocholesterolemic (NC n=7), fed with normal chow (S11, Purina, St Luis, MO) and hypercholesterolemic (HC n=7), fed a high fat/high cholesterol chow (Sinclair Research Center, Inc. Columbia, MO) from age 16 to 20 weeks. Animal weight was evenly matched between the two groups (NC 22.4±1.3 kg vs. HC 21.4±0.9 kg, p=0.5).

Animals were housed individually and provided with laboratory chow and water. All experiments were approved by the BIDMC IACCUC and conformed to the US National Institutes of Health guidelines regulating the care and use of laboratory animals (NIH publication 5377-3, 1996).

Surgical Protocol

Pigs were sedated with Telazol and weighed before induction of anesthesia (4 mg/kg, IM) followed by endotracheal intubation and ventilation with a volume-cycled ventilator (North American Dragger, Telford, PA). Anesthesia was established and maintained with 2.0% isoflurane (Ultane; Abbott Laboratories). The right common femoral artery was used for arterial blood sampling and continuous monitoring of intra-arterial blood pressure (Millar Instruments, Houston, TX). Arterial blood gas analysis, hematocrit, and core temperature were assessed every 30 minutes. Prior to left anterior descending (LAD) coronary artery occlusion, each animal received a one liter bolus of Lactated Ringer's solution followed by continuous infusion (15 ml/kg/hour). A phenylephrine drip (0.25 µg/kg/min) to prevent hypotension

induced by isoflurane, heparin (80 units/kg bolus), and lidocaine (1.5 mg/kg) to control ventricular dysrhythmia, were administered. A median sternotomy was performed. A catheter-tipped manometer (Millar Instruments, Houston, TX) was introduced through the apex of the left ventricle (LV) to record LV pressure. The LAD was occluded 3 mm distal to the origin of the second diagonal branch by a Rommel tourniquet. After 60 min of ischemia the tourniquet was released and the myocardium was reperfused for 120 min. LAD flow was monitored by a transonics Doppler probe. At the end of reperfusion the LAD was religated and monastryl blue pigment (Engelhard Corp, Louisville, KY) was injected into the aortic root to demarcate the area at risk (AAR). The heart was rapidly excised and sliced into 1cm-thick slices perpendicular to the LAD up to the area of ligation. Tissue from the second slice was used in molecular and coronary microvascular reactivity studies. The remaining tissue was incubated in 1% triphenyl tetrazolium chloride (TTC; Sigma Chemical Co, St Louis, MO) solution for 30 min and infarct size was assessed as previously described¹². Ventricular dysrhythmia (ventricular fibrillation or pulseless ventricular tachycardia) events were recorded and treated with immediate electrical cardioversion with 20–50 J.

Measurement of Global and Regional Myocardial Function

Indices of global and regional myocardial function were monitored and recorded during the entire experiment: mean arterial pressure (MAP); developed LV pressure (DLVP); positive (+dP/dt) and negative (–dP/dt) first derivatives of LV pressure; longitudinal and horizontal segmental shortening (SS) in the AAR, for 10 sequential beats at baseline and then every 30 minutes (Occlusion-O1 30 min and O2 60 min; Reperfusion- R1 30, R2 60, R3 90, and R4 120 minutes) using a Sonometrics system (Sonometrics Corp. London, ON, Canada) as previously described¹³.

Quantification of Myocardial Infarct Size

Heart slices (1cm-thick) were incubated in 1% TTC solution as previously described¹³. Briefly, necrotic (pale), the AAR (bright red), and non-ischemic portion of the heart specimens (purple) were photographed and measured. The size of the AAR and percent necrosis in the AAR was calculated in each individual slice by planimetry (Image J 1.4, INH, Bethesda, MD) using the following equations: $[(LV \text{ necrosis surface area} + \text{non-infarct AAR surface area}) / LV \text{ total surface} \times 100]$ and $[(LV \text{ necrosis surface area} / LV \text{ AAR surface area}) \times 100]$.

Coronary Microvascular Reactivity Studies

Coronary microvascular reactivity was examined in the ischemic territory as previously described¹³. Briefly, coronary arterioles (80 to 130 μm) were dissected with a 40 \times microscope. Microvessels were mounted on dual glass micropipettes and examined in a pressurized isolated microvessel chamber. Adenosine diphosphate (ADP, 1 nM to 100 μM), substance P (0.1 pM to 10 nM), A23187 (1 nM to 10 μM), and sodium nitroprusside (SNP, 1 nM to 100 μM) were applied extra-luminally after pre-contraction by 20–50% of the baseline diameter with the thromboxane A2 analog U46619 (0.1–1 μM).

Western Blotting

Myocardial samples were homogenized in RIPA buffer (Boston Bioproducts, Worcester, MA) and protein concentration was determined by BCA assay (Pierce, Rockford, Illinois). Equal amounts of lysate were subjected to SDS-Page and immunoblotting as previously described¹³. Primary antibodies were used according to the manufacturer's recommendation. Levels of Bcl-2, caspase-3, cleaved caspase-3 (Asp175), PARP, cleaved PARP(Asp214), Akt and phospho-Akt(Ser473), BNip3, eNOS and phospho-eNOS(Ser1177), PKC ϵ and phospho-pan-PKC(ϵ ,Ser729), p38 MAPK and phospho-p38(Thr180/Tyr182) (Cell Signaling Technology, Beverly, MA), Erk 1/2 and phospho-Erk 1/2(Thr185/Tyr187) (Invitrogen. Carlsbad, CA),

myeloperoxidase (Dako, Carpinteria, CA) were assessed. Immunoblotting for vinculin was used to confirm equal protein loading (Santa Cruz Biothechnology, Inc. Santa Cruz, CA). Band intensities were normalized to Ponceau staining intensity. Data are presented as mean±SEM in arbitrary density units (AU).

Protein Oxidation and Lipid Peroxidation

Protein oxidation (OxyBlot™, Chemicon International, Inc. Temecula, CA) and lipid peroxidation (Peroxidation colorimetric microplate assay, Oxford Biomedical Research, Oxford, MI) in myocardial samples were measured according to the manufacturer's recommendation. Data analyzed using Student's t-test.

Nitrotyrosine Staining

Formalin-fixed paraffin embedded heart tissue was processed as previously described¹⁴ (four slides from each group, non-ischemic and ischemic territories) and was incubated overnight at 4°C with monoclonal nitrotyrosine antibody (USBiological, Swampscott, MA). Data analyzed using Student's t-test.

TUNEL Staining

Apoptotic cells were identified using the ApopTag detection kit according to manufacturer's specifications (Chemicon Inc, Temecula, CA). At least one cm² of tissue from the AAR was analyzed from each animal (4 per group). The number of TUNEL-positive cardiomyocytes is expressed as positive cells/cm². Data analyzed using Student's t-test.

Serum Lipid Profile

Serum lipid profile was measured by Siemens Advia 1200 chemistry system (Accell Inc. Quebec, Canada). Data are presented as mean±SEM and were analyzed using Student's t-test.

Statistical Analysis

Functional and microvascular reactivity data were analyzed using repeated measures ANOVA. Infarct size and western blot densitometry were analyzed using unpaired Student's t-test. The incidence of VT/VF was analyzed using Chi-square test. Western blot data between the HC vs. NC groups were compared within the same myocardial territory (either non-ischemic or ischemic territories). Data are reported as mean±SEM and p<.05 was considered significant (Systat, San Jose, CA).

Results

Serum Lipid Profile

Levels of total serum cholesterol (13.8±1.8 vs. 1.5±0.3 mmol/L, p<.05), D-LDL (5.5±0.7 vs. 0.5±0.04 mmol/L, p<.05) and D-HDL (1.8±0.1 vs. 0.5±0.05 mmol/L, p<.05) were significantly higher in pigs fed a high fat/high cholesterol chow compared to those fed a normal chow. The level of triglycerides (0.3±0.03 vs. 0.3±0.1 mmol/L, p=0.67) was not different between groups.

Myocardial Infarct Size

While the AAR was similar between groups (Figure 1A), the area of necrosis was 45% greater in the HC vs. NC (Figure 1B). Transmural necrosis involving the LV wall and septum was present in 7/7 HC pigs but only in 4/7 NC pigs (Figure 1C/D, arrows).

Arterial Blood Gas, Hematocrit, Core Temperature, and Hemodynamic Parameters

There were no difference among groups at any time point with respect to arterial blood gas, hematocrit, and core temperature.

Heart rate ($p=0.5$) and LAD flow ($p=0.4$) were similar between groups at all recorded time points. LAD blood flow increased 2.8 fold during the first minute of reperfusion (hyperemic response) and then steadily declined to reach the baseline levels by the end of the experiment in both groups. There was a trend toward higher mean arterial pressure (MAP) and higher developed left ventricular pressure (DLVP) in the HC group (Figure 2A/B).

Global and Regional Myocardial Function

Global systolic LV function, as determined by $+dP/dt$ was greater in the HC group vs. NC group. There was no significant difference in $-dP/dt$ between groups (Figure 2C/D). Segmental shortening (SS) in the horizontal axis was significantly decreased in HC animals beginning 1 hour into reperfusion (Figure 2E), while no difference was observed in the longitudinal axis (Figure 2F).

Incidence of VF/VT

VF/VT requiring cardioversion tended to be higher in the HC group vs. NC group. (5 out of 7 vs. 2 out of 7, $p=0.37$). Generally, VF/VT appeared earlier in the ischemic period in the HC group compared to the NC group, in which it appeared early into reperfusion. All ventricular dysrhythmias were successfully terminated with electrical cardioversion.

Coronary Microvessel Function

There were no significant differences between groups in endothelial-dependent and -independent relaxation of microvessels taken from the ischemic territory (Figure 3A/B/C/D).

Myocardial Oxidative Stress Indicators

Protein oxidation (Figure 4A) and lipid peroxidation (Figure 4B) were higher in the HC group vs. NC group in the ischemic territory only. Nitrotyrosine staining in the ischemic territory was also more intense in the HC group (Figure 4C), but not in the non-ischemic territory. While the expression of eNOS in the ischemic territory was similar between groups (NC 0.01 ± 0.002 vs. 0.01 ± 0.002 AU, $p=0.1$), the expression of phospho-eNOS (Ser1177) was higher in the HC group (Figure 4D).

Profile of Pro-inflammatory Proteins

Myeloperoxidase (MPO) expression was higher in the HC group vs. NC group in the non-ischemic myocardium. There was a trend of lower MPO expression ($p=0.097$) in the ischemic territory (Figure 5A). The expression of p38 was higher in the HC group vs. NC group in both territories (Figure 5B). The expression of phospho-p38(Thr180/Tyr182) was higher in the HC group in the non-ischemic territory (Figure 5C), whereas no bands of phospho-p38 was seen in the ischemic territory in either group.

Profile of Pro-Apoptotic Signaling Proteins

Total PARP expression was higher in the HC group vs. NC group in both territories (Figure 6A). However, cleaved PARP(Asp214) expression was lower in the HC group (non-ischemic and ischemic territories) (Figure 6B). The expression of total caspase-3 and its active form, cleaved caspase-3(Asp175) was not different between two groups in both territories (Figure 6C/D). The expression of BNip3 was higher in the HC group in the non-ischemic territory, but was similar in the ischemic territory (Figure 6E).

Profile of Pro-Survival Signaling Proteins

The expression of anti-apoptotic Bcl-2 was lower in the HC group in both territories (Figure 6F). Total Akt expression was lower in the HC group compared to the NC group in the ischemic territory. The expression of phospho-Akt(Ser473) was higher in the non-ischemic territory, but lower in the ischemic territory in the HC group (Figure 7A/B). The expression of total Erk 1/2 was higher in the HC group in both territories (Figure 7C). The expression of phospho-Erk 1/2 (Thr185/Tyr187) was higher in the non-ischemic territory in the HC group, but similar in the ischemic territory (Figure 7D). The expression of PKC ϵ was not different between groups in neither the non-ischemic nor the ischemic territories, whereas the expression of phospho-PKC ϵ (Ser729) was higher in the non-ischemic territory and lower in the ischemic territory in the HC group (Figure 7E/F). All western blot data from the non-ischemic and the ischemic myocardium are summarized in table 1 and table 2, respectively (See Online Supplemental Data).

TUNEL Staining for Apoptosis

The apoptotic cell counts in the AAR was 3.8 fold higher in the HC compare to NC (59.5 ± 14.9 cells/cm² vs. 15.7 ± 4.3 cells/cm², $p < .05$). Most apoptotic cells were cardiomyocytes and mainly located near the necrotic area.

Discussion

Despite many advances in basic science and treatment options, the majority of patients with CAD have elevated cholesterol levels¹⁵. Clinical studies to assess the effect of hypercholesterolemia on myocardial IR have been conducted in the setting of multiple coexisting risk factors¹⁶, while in rabbit and rodent IR models, the effect of hypercholesterolemia has yielded varying and controversial results¹⁰. The principal finding of this study was that hypercholesterolemia alone increased myocardial necrosis by 45% over what was observed in the NC animals. This may be explained by increased inflammation and oxidative stress in the setting of hypercholesterolemia, as has been reported in previous studies¹⁷. This is corroborated in our study by increased indices of oxidative stress in the ischemic myocardium such as protein oxidation, lipid peroxidation, and nitrotyrosylation during IR. Our findings accentuate the importance of antioxidant therapy¹⁸ as a potential strategy to protect the myocardium before re-establishing reperfusion in hypercholesterolemic patients^{13,19}.

A novel finding in this study was that hypercholesterolemia increased baseline indices of myocardial function. The higher peak +dP/dt, which is a good index of ventricular performance not influenced by afterload, wall motion abnormalities, or variations in ventricular anatomy and morphology, demonstrated that hypercholesterolemia had a positive inotropic effect. The dietary abundance of short chain fatty acids, which are a primary energy source for cardiomyocytes²⁰ may partially explain this hyperdynamic function seen in the HC group. This also may lead to increased myocardial oxygen demand and intensify myocardial injury during hypoxia. In contrast, a previous study showed no differences with respect to myocardial function and myocardial necrosis size between normocholesterolemic control and hypercholesterolemic control pigs in the setting of 3 hrs ischemia and 2 hrs of reperfusion¹¹. Other important finding was that myocardial necrosis size was high in both groups, above 98%¹¹. In our study after 1 hr of ischemia and 2 hrs of reperfusion only 61% of AAR becomes necrotic in the hypercholesterolemic animals vs. 42% in the normocholesterolemic. Thus finding from our study accentuate the importance of early reperfusion in patients with hypercholesterolemia following AMI. The majority of previously reported data from small animal models demonstrated that hypercholesterolemia has either a negative inotropic effect or no difference on basal contractile state^{21,22}. Moreover, the hyperdynamic pattern and extent of necrosis seen in the HC was also associated with increased and an earlier onset of VF/VT

during ischemia. Though this finding warrants further investigation, it may support the need for aggressive prevention of ventricular arrhythmia during AMI in hypercholesterolemic patients.

Surprisingly, there were no differences in microvascular relaxation between control and hypercholesterolemic pigs. Numerous animal and clinical models have reported impaired endothelium-dependent and -independent relaxation in the setting of hypercholesterolemia, and have implied that this may predispose to increased IR injury²³. In our study, coronary microvascular relaxation was only examined in the ischemic territory. IR is well known to result in significant impairments in coronary microvascular relaxation²⁴. Therefore, it is likely that the microvascular injury sustained by IR was sufficient to veil any functional differences in relaxation due to the addition of hypercholesterolemia.

The detrimental role of oxidative stress on the myocardium in the setting of hypercholesterolemia has long been established in the literature^{14, 25}. However, the magnitude of damage conferred by oxidative stress on the ischemic myocardium during IR injury is not well studied. While some studies have shown that increased oxidative stress is associated with higher expression of MPO in ischemic myocardium⁵, in this study increased oxidative stress in the ischemic myocardium was associated with lower expression of MPO after IR. In addition, previous reports conducted in rabbit models have demonstrated that hypercholesterolemia is associated with lower NO production due to lower phosphorylation of eNOS in the heart²⁶. We found that hypercholesterolemia indeed induces phospho-eNOS in the ischemic myocardium. Coupled with increased nitrotyrosine staining, this suggests that hypercholesterolemia-induced oxidant formation and eNOS activation may promote peroxynitrite formation.^{27, 28} In addition to hypercholesterolemia-induced oxidative stress, our previous work highlighted a role for increased oxidative stress in normocholesterolemic swine treated with high-dose atorvastatin²⁹. If indeed, hypercholesterolemia increases infarct size via enhanced oxidative stress pathway, it would be of value to evaluate these endpoints in a statin-treated hypercholesterolemia model with acute ischemia to determine if there is a greater exacerbation of the ischemic insult.

Recently p38 MAPK has emerged as an important mediator of inflammatory signals and apoptosis during IR injury and its inhibition has been shown to be cardioprotective³⁰. In this study hypercholesterolemia was associated with a noticeable overexpression of p38 MAPK in both the ischemic and non-ischemic myocardium, and a higher level of activation in the non-ischemic territory. Taken together, the MPO and p38 MAPK data strongly suggest that hypercholesterolemia induces higher basal levels of inflammation in the myocardium, which may prime it for increased IR injury.

Free oxygen radicals and inflammation are also known to promote apoptotic pathways and may be associated with the increase in pro-apoptotic signaling including PARP, caspase 3, and BNip-3 in the HC pigs seen in this study⁸. Furthermore, hypercholesterolemia was associated with reduced Bcl-2 expression, which is known to have antioxidant properties and may instigate greater oxidant dependent damage with acute IR. In addition, Bcl-2 plays a crucial role in preventing apoptosis, by blocking the activation of executioner caspases 3, 6, and 7³¹, and the release of mitochondrial cytochrome c³². Although IR-related cardiomyocyte death is traditionally assumed to be necrotic, this and other studies have shown that a substantial proportion of cardiomyocytes deaths are apoptotic³³.

Finally, we found a decrease in the expression of most pro-survival proteins in the HC group in the myocardial territory subjected to IR. Total Akt, phospho-Akt, and phospho-PKC ϵ were all significantly decreased in the ischemic myocardium in the HC group compared to the NC group. When activated Akt serves many pro-survival functions in cardiomyocytes, including

the prevention of apoptosis³⁴, and the decreased total expression and phosphorylation at serine 473 residue may also diminish cardiomyocyte survival following IR in the setting of hypercholesterolemia. PKC ϵ has been shown to have an important role in postconditioning cardioprotection via phosphorylation of Akt and Erk 1/2, activation of mitochondrial K_{ATP} channel^{35,36}. This may explain the previously reported finding that preconditioning and postconditioning fail to reduce the area of myocardial necrosis in the hypercholesterolemic pigs in the setting of IR injury¹¹. Interestingly, the non-ischemic territory displayed a very different signaling profile, with hypercholesterolemia inducing higher expression of phospho-Akt, phospho-Erk 1/2, and phospho-PKC ϵ .

In conclusion, hypercholesterolemia alone increased the susceptibility of the myocardium to infarction in the setting of acute IR. The hyperdynamic state, increased myocardial oxidative stress and inflammation, attenuation of cell-survival pathways, and induction of apoptosis may account for the further expansion of myocardial necrosis and the deterioration of regional cardiac function during IR in the setting of hypercholesterolemia.

Limitations

While providing important functional and molecular data about the role of hypercholesterolemia in acute IR, this study has several limitations. First, It should be noted that all of the control tissue was from the non-ischemic territory, however, it cannot be ruled out that ischemic insult may affect signaling in remote heart, including potential inflammatory insult and release of soluble mediators from the infarcted myocardium. Second our time course for tissue harvest (3 hours after the onset of ischemia) could not account for the long-term effects of hypercholesterolemia on myocardial function and apoptosis. Finally, only a short-term diet induction of hypercholesterolemia was performed. Although this model is adept at examining changes in AMI due to hypercholesterolemia alone, the chronic secondary effects of hypercholesterolemia may not be developed at this time point. Whether this is similar to long-standing endogenous or exogenous hypercholesterolemia in patients needs to be further evaluated.

Supplementary Material

Refer to Web version on PubMed Central for supplementary material.

Acknowledgements

We thank BIDMC Animal Research Facility staff for their efforts.

Funding

Funding for this project was provided to Dr. F.W.S by NHLBI (RO1 HL46716, HL69024, and HL85647), OrthoLogic Corp, and NIH T32-HL076130 (R.M.O, R.T.C, M.P.R) and the Irving Bard Memorial Fellowship (R.M.O, M.P.R).

References

1. Murray CJ, Lopez AD. Alternative projections of mortality and disability by cause 1990–2020: Global Burden of Disease Study. *Lancet* 1997;349:1498–1504. [PubMed: 9167458]
2. Corti R, Fuster V, Badimon JJ, Hutter R, Fayad ZA. New understanding of atherosclerosis (clinically and experimentally) with evolving MRI technology in vivo. *Ann N Y Acad Sci* 2001;947:181–195. [PubMed: 11795266]discussion 195-188
3. Ballantyne CM, Olsson AG, Cook TJ, Mercuri MF, Pedersen TR, Kjekshus J. Influence of low high-density lipoprotein cholesterol and elevated triglyceride on coronary heart disease events and response to simvastatin therapy in 4S. *Circulation* 2001;104:3046–3051. [PubMed: 11748098]

4. Prasad K, Kalra J. Experimental atherosclerosis and oxygen free radicals. *Angiology* 1989;40:835–843. [PubMed: 2764311]
5. Liu HR, Tao L, Gao E, Qu Y, Lau WB, Lopez BL, Christopher TA, Koch W, Yue TL, Ma XL. Rosiglitazone inhibits hypercholesterolaemia-induced myeloperoxidase upregulation—a novel mechanism for the cardioprotective effects of PPAR agonists. *Cardiovasc Res* 2009;81:344–352. [PubMed: 19010810]
6. Prasan AM, McCarron HC, Zhang Y, Jeremy RW. Myocardial release of nitric oxide during ischaemia and reperfusion: effects of L-arginine and hypercholesterolaemia. *Heart Lung Circ* 2007;16:274–281. [PubMed: 17420156]
7. Golino P, Maroko PR, Carew TE. The effect of acute hypercholesterolemia on myocardial infarct size and the no-reflow phenomenon during coronary occlusion-reperfusion. *Circulation* 1987;75:292–298. [PubMed: 3791611]
8. Wang TD, Chen WJ, Su SS, Lo SC, Lin WW, Lee YT. Increased cardiomyocyte apoptosis following ischemia and reperfusion in diet-induced hypercholesterolemia: relation to Bcl-2 and Bax proteins and caspase-3 activity. *Lipids* 2002;37:385–394. [PubMed: 12030319]
9. Wang S, El-Deiry WS. TRAIL and apoptosis induction by TNF-family death receptors. *Oncogene* 2003;22:8628–8633. [PubMed: 14634624]
10. Thim T, Bentzon JF, Kristiansen SB, Simonsen U, Andersen HL, Wassermann K, Falk E. Size of myocardial infarction induced by ischaemia/reperfusion is unaltered in rats with metabolic syndrome. *Clin Sci (Lond)* 2006;110:665–671. [PubMed: 16448385]
11. Zhao JL, Yang YJ, You SJ, Cui CJ, Gao RL. Different effects of postconditioning on myocardial no-reflow in the normal and hypercholesterolemic mini-swines. *Microvasc Res* 2007;73:137–142. [PubMed: 17055004]
12. Toyoda Y, Di Gregorio V, Parker RA, Levitsky S, McCully JD. Anti-stunning and anti-infarct effects of adenosine-enhanced ischemic preconditioning. *Circulation* 2000;102:III326–III331. [PubMed: 11082409]
13. Sodha NR, Clements RT, Feng J, Liu Y, Bianchi C, Horvath EM, Szabo C, Sellke FW. The effects of therapeutic sulfide on myocardial apoptosis in response to ischemia-reperfusion injury. *Eur J Cardiothorac Surg* 2008;33:906–913. [PubMed: 18314343]
14. Mannheim D, Versari D, Daghini E, Gossel M, Galili O, Chade A, Rajkumar VS, Ritman EL, Lerman LO, Lerman A. Impaired myocardial perfusion reserve in experimental hypercholesterolemia is independent of myocardial neovascularization. *Am J Physiol Heart Circ Physiol* 2007;292:H2449–H2458. [PubMed: 17208989]
15. Nag SS, Daniel GW, Bullano MF, Kamal-Bahl S, Sajjan SG, Hu H, Alexander C. LDL-C goal attainment among patients newly diagnosed with coronary heart disease or diabetes in a commercial HMO. *J Manag Care Pharm* 2007;13:652–663. [PubMed: 17970603]
16. Galinanes M, Fowler AG. Role of clinical pathologies in myocardial injury following ischaemia and reperfusion. *Cardiovasc Res* 2004;61:512–521. [PubMed: 14962481]
17. Inagi R. Oxidative stress in cardiovascular disease: a new avenue toward future therapeutic approaches. *Recent Patents Cardiovasc Drug Discov* 2006;1:151–159.
18. Rosa CE, Bianchini A, Monserrat JM. Antioxidant responses of *Laonereis acuta* (Polychaeta) after exposure to hydrogen peroxide. *Braz J Med Biol Res* 2008;41:117–121. [PubMed: 18297192]
19. Zhang Y, Shi G, Zheng J, Tang Z, Gao P, Lv Y, Guo F, Jia Q. The protective effects of N-n-butyl haloperidol iodide on myocardial ischemia-reperfusion injury in rats by inhibiting Egr-1 overexpression. *Cell Physiol Biochem* 2007;20:639–648. [PubMed: 17762190]
20. Labarthe F, Gelinas R, Des Rosiers C. Medium-chain Fatty Acids as Metabolic Therapy in Cardiac Disease. *Cardiovasc Drugs Ther.* 2008
21. Osborne JA, Lento PH, Siegfried MR, Stahl GL, Fusman B, Lefer AM. Cardiovascular effects of acute hypercholesterolemia in rabbits. Reversal with lovastatin treatment. *J Clin Invest* 1989;83:465–473. [PubMed: 2913050]
22. Hoshida S, Yamashita N, Otsu K, Kuzuya T, Hori M. Cholesterol feeding exacerbates myocardial injury in Zucker diabetic fatty rats. *Am J Physiol Heart Circ Physiol* 2000;278:H256–H262. [PubMed: 10644606]

23. Kawashima S, Yokoyama M. Dysfunction of endothelial nitric oxide synthase and atherosclerosis. *Arterioscler Thromb Vasc Biol* 2004;24:998–1005. [PubMed: 15001455]
24. Piana RN, Shafique T, Dai HB, Sellke FW. Epicardial and endocardial coronary microvascular responses: effects of ischemia-reperfusion. *J Cardiovasc Pharmacol* 1994;23:539–546. [PubMed: 7516002]
25. Besse S, Bulteau AL, Boucher F, Riou B, Swynghedauw B, de Leiris J. Antioxidant treatment prevents cardiac protein oxidation after ischemia-reperfusion and improves myocardial function and coronary perfusion in senescent hearts. *J Physiol Pharmacol* 2006;57:541–552. [PubMed: 17229980]
26. Onody A, Csonka C, Giricz Z, Ferdinandy P. Hyperlipidemia induced by a cholesterol-rich diet leads to enhanced peroxynitrite formation in rat hearts. *Cardiovasc Res* 2003;58:663–670. [PubMed: 12798440]
27. Schulz R, Wambolt R. Inhibition of nitric oxide synthesis protects the isolated working rabbit heart from ischaemia-reperfusion injury. *Cardiovasc Res* 1995;30:432–439. [PubMed: 7585835]
28. Cai H, Harrison DG. Endothelial dysfunction in cardiovascular diseases: the role of oxidant stress. *Circ Res* 2000;87:840–844. [PubMed: 11073878]
29. Sodha NR, Boodhwani M, Ramlawi B, Clements RT, Mieno S, Feng J, Xu SH, Bianchi C, Sellke FW. Atorvastatin increases myocardial indices of oxidative stress in a porcine model of hypercholesterolemia and chronic ischemia. *J Card Surg* 2008;23:312–320. [PubMed: 18598320]
30. Jaswal JS, Gandhi M, Finegan BA, Dyck JR, Clanachan AS. Inhibition of p38 MAPK and AMPK restores adenosine-induced cardioprotection in hearts stressed by antecedent ischemia by altering glucose utilization. *Am J Physiol Heart Circ Physiol* 2007;293:H1107–H1114. [PubMed: 17496214]
31. Okamura T, Miura T, Takemura G, Fujiwara H, Iwamoto H, Kawamura S, Kimura M, Ikeda Y, Iwatate M, Matsuzaki M. Effect of caspase inhibitors on myocardial infarct size and myocyte DNA fragmentation in the ischemia-reperfused rat heart. *Cardiovasc Res* 2000;45:642–650. [PubMed: 10728385]
32. Gustafsson AB, Gottlieb RA. Bcl-2 family members and apoptosis, taken to heart. *Am J Physiol Cell Physiol* 2007;292:C45–C51. [PubMed: 16943242]
33. Zhao ZQ, Nakamura M, Wang NP, Wilcox JN, Shearer S, Ronson RS, Guyton RA, Vinten-Johansen J. Reperfusion induces myocardial apoptotic cell death. *Cardiovasc Res* 2000;45:651–660. [PubMed: 10728386]
34. Fujio Y, Nguyen T, Wencker D, Kitsis RN, Walsh K. Akt promotes survival of cardiomyocytes in vitro and protects against ischemia-reperfusion injury in mouse heart. *Circulation* 2000;101:660–667. [PubMed: 10673259]
35. Costa AD, Garlid KD, West IC, Lincoln TM, Downey JM, Cohen MV, Critz SD. Protein kinase G transmits the cardioprotective signal from cytosol to mitochondria. *Circ Res* 2005;97:329–336. [PubMed: 16037573]
36. Murphy E, Steenbergen C. Mechanisms underlying acute protection from cardiac ischemia-reperfusion injury. *Physiol Rev* 2008;88:581–609. [PubMed: 18391174]

Abbreviations

IR, myocardial-ischemia reperfusion injury
 NC, normocholesterolemic
 HC, hypercholesterolemic
 AAR, area at risk (ischemic)
 LAD, left anterior descending coronary artery
 LV, left ventricle
 PARP, poly ADP ribose polymerase
 Bcl 2, B-cell lymphoma 2
 BNip 3, Bcl2/adenovirus E1B 19 kDa-interacting protein
 eNOS, endothelial nitric oxide synthase
 PKCε, protein kinase c-epsilon
 Erk 1/2, extracellular signal-regulated kinase
 p38 MAPK, mitogen activated protein kinase

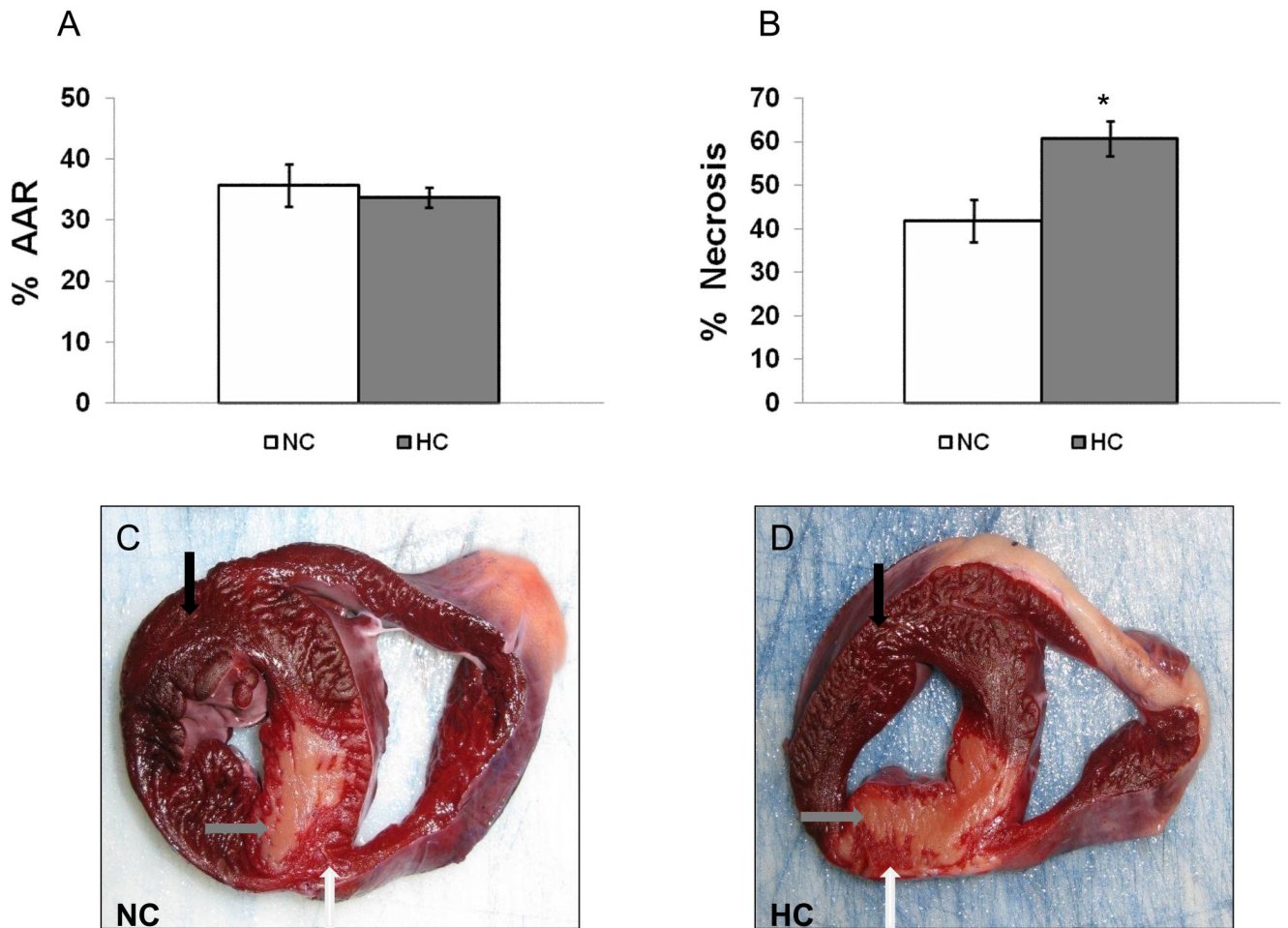


Figure 1.

A) Percent of LV wall area at the risk (AAR) ($p=0.6$) and B) necrosis of AAR in the NC and HC animals. Shown are representative images of the myocardium after TTC staining in NC (C) and HC (D). Black arrow pointed to the non-ischemic (purple), white arrow to AAR (bright red), and gray arrow to the necrotic area (pale). Data presented as mean \pm SEM and compare NC ($n=7$) and HC ($n=7$) groups. * $p<.05$

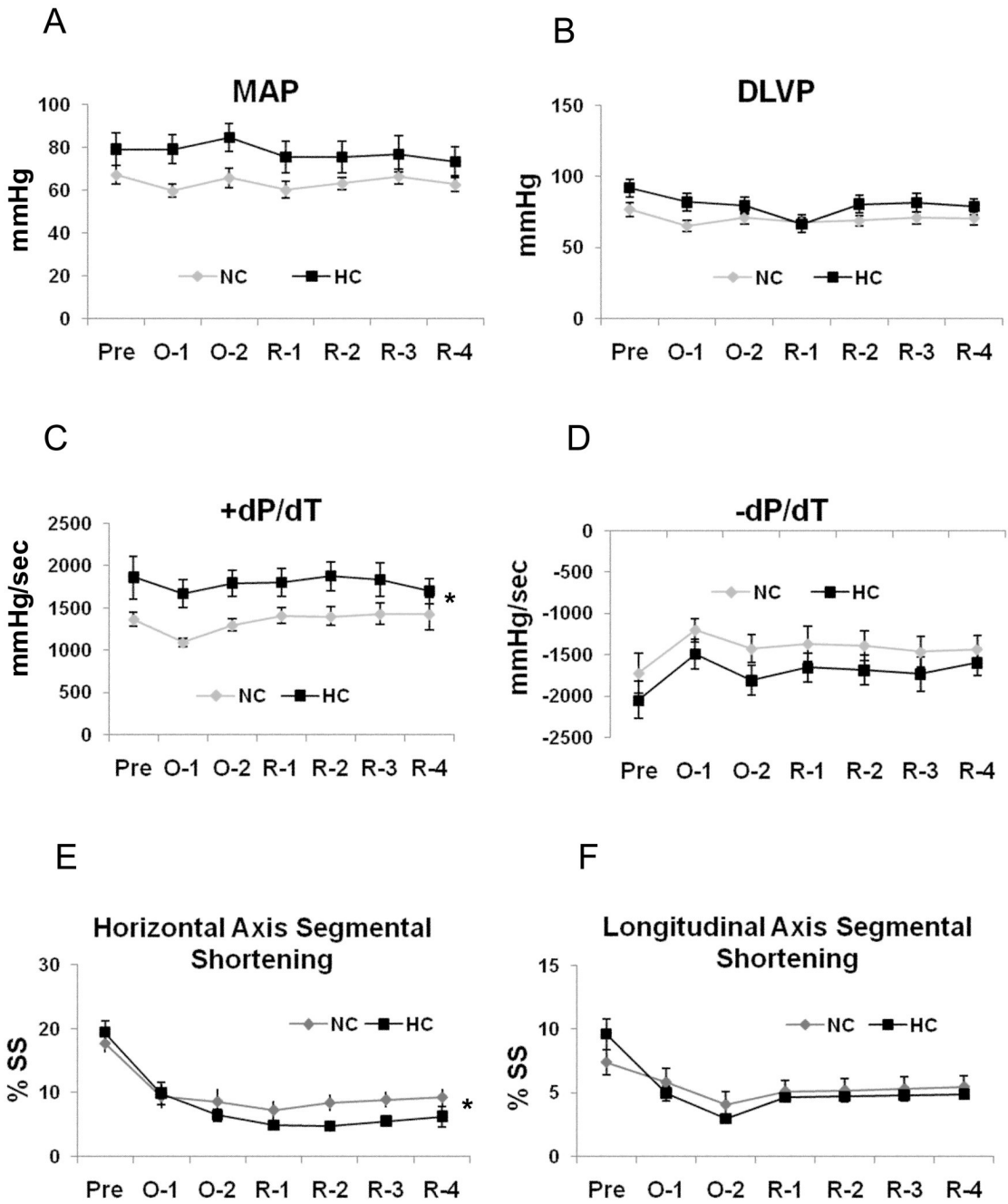


Figure 2. Global and regional left ventricular function: A) Mean arterial pressure (MAP, $p=.08$), B) Developed left ventricular pressure (DLVP, $p=.08$), C) Positive first order derivative of ventricular pressure (+dP/dt), D) Negative first order derivative of ventricular pressure (-dP/dt, $p=.08$), E) Percent of segmental shortening (SS) in horizontal axis, and F) Percent of SS in longitudinal axis ($p=0.4$). Baseline- Pre, 30 and 60 minutes into ischemia/LAD occlusion-O1/O2, R1-30, R2-60, R3-90 and R4-120 minutes into reperfusion. Data presented as mean±SEM and compare NC (n=7) and HC (n=7) groups. * $p<.05$

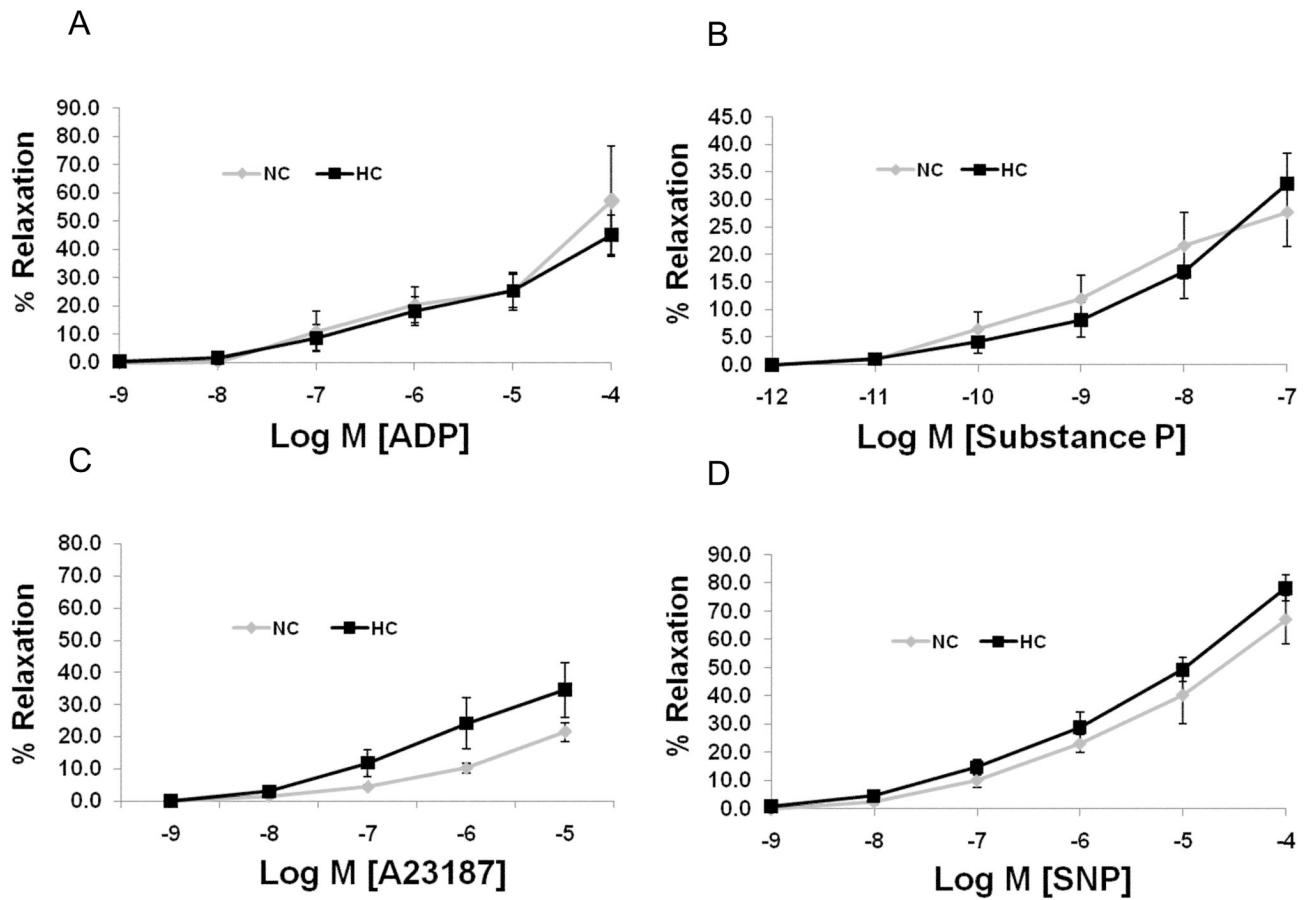


Figure 3. Microvascular responses to endothelium-dependent agents: A) adenosine diphosphate (ADP, $p=0.7$), B) Substance P ($p=0.8$), and C) Ca^{2+} ionophore A23187 ($p=0.2$), D) Microvascular response to endothelium-independent agent sodium nitroprusside (SNP, $p=0.2$). Data presented as percent of relaxation and compare NC ($n=7$) and HC ($n=7$) groups.

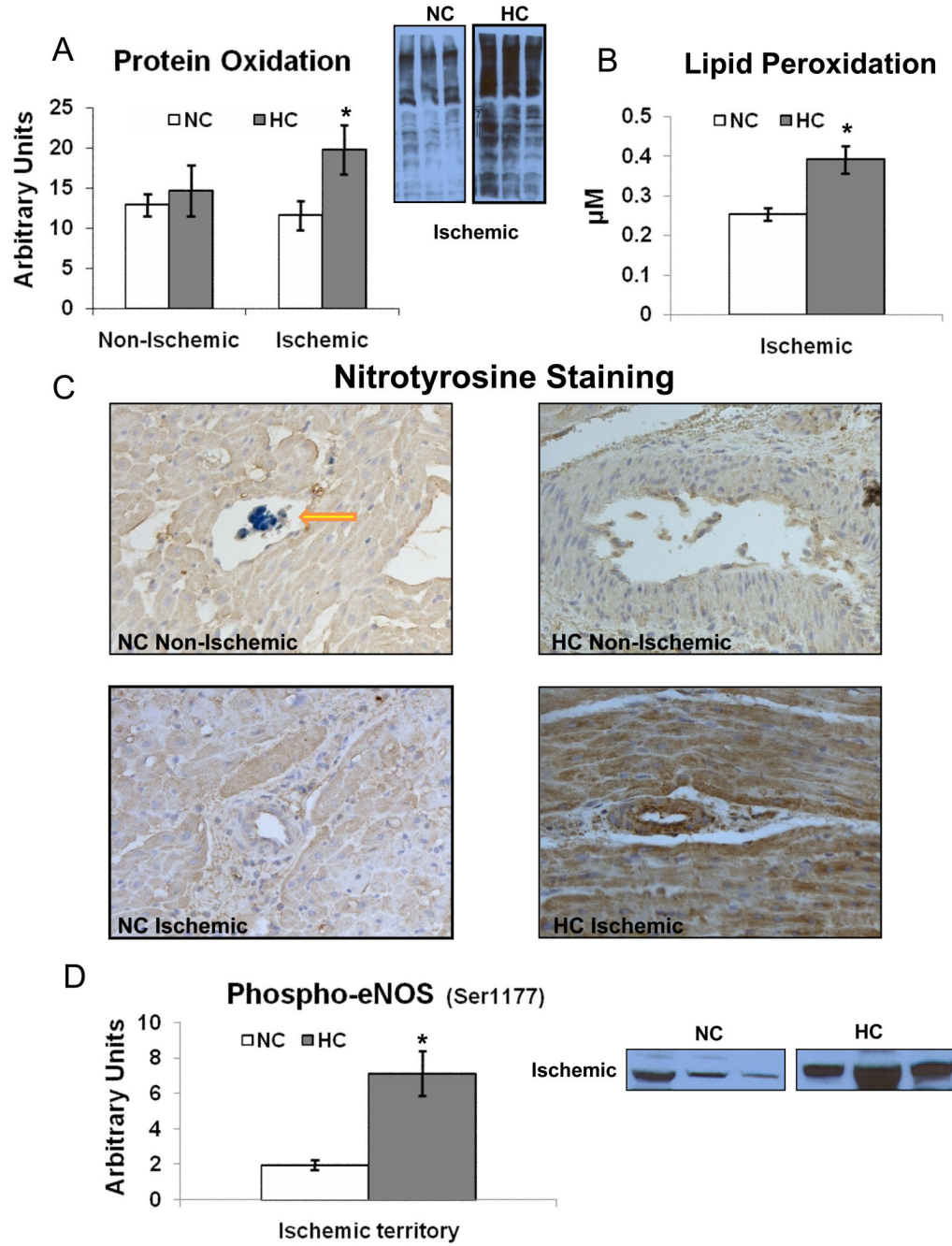


Figure 4. Myocardial oxidative stress indices: A) Protein oxidation (1.7 fold increased in the HC vs. NC), B) Lipid peroxidation (1.4 fold increased in the HC vs. NC) in the ischemic territory, and C) Nitrotyrosine staining. The HC samples have more intense nitrotyrosine staining (brown) in the ischemic territory. Yellow arrow denotes monastryl blue pigment in the capillary in the non-ischemic territory. (Original magnification $\times 20$), D) Expression of phospho-eNOS (Ser1177) in the ischemic territory. Representative western blots (insets, 3 samples from each group) are shown. Data compare NC (n=7) and HC (n=7) groups. * $p < .05$

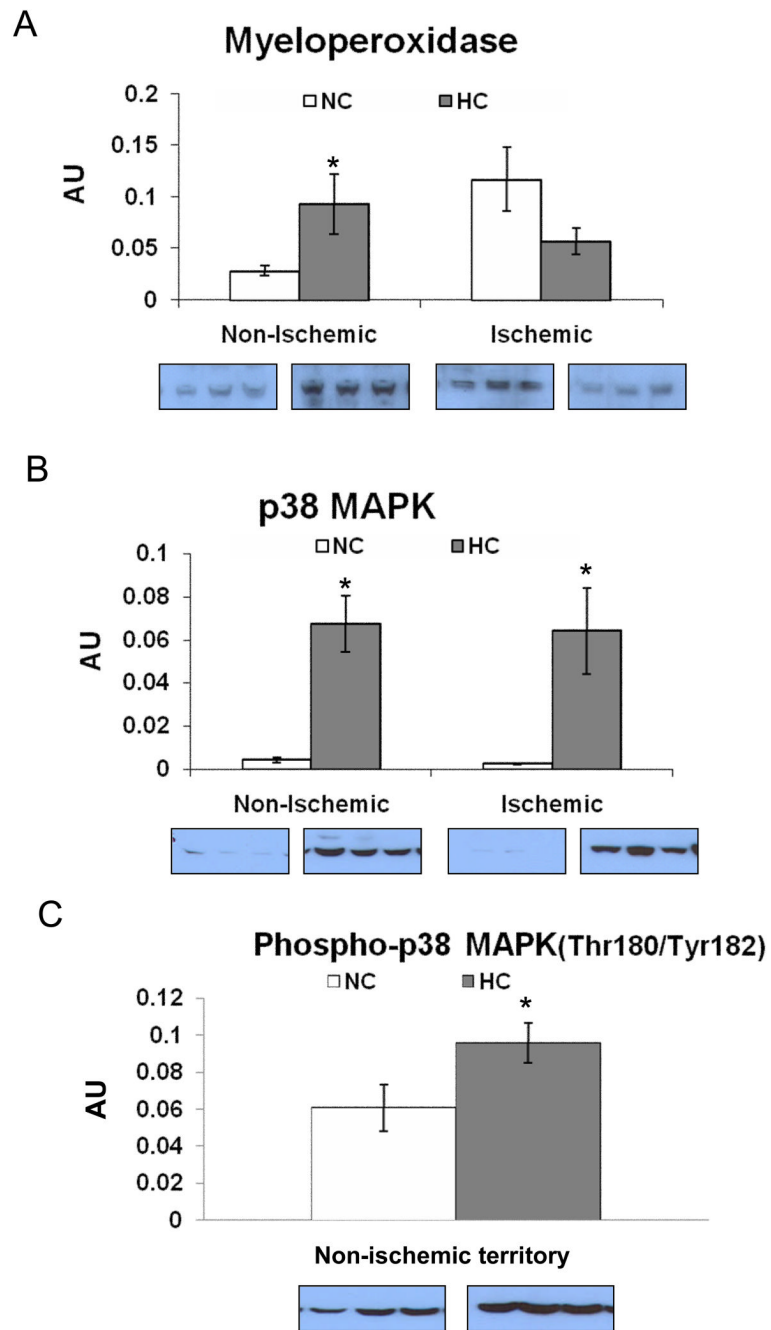


Figure 5. The expression of pro-inflammatory proteins: A) Myeloperoxidase, B) p38-MAPK and C) Phospho-p38 MAPK(Thr180/Tyr182) in the non-ischemic territory. Representative western blots (insets, 3 samples from each group) are shown. Data presented as mean \pm SEM in arbitrary density units (AU) and compare NC (n=7) and HC (n=7) groups. * p<.05

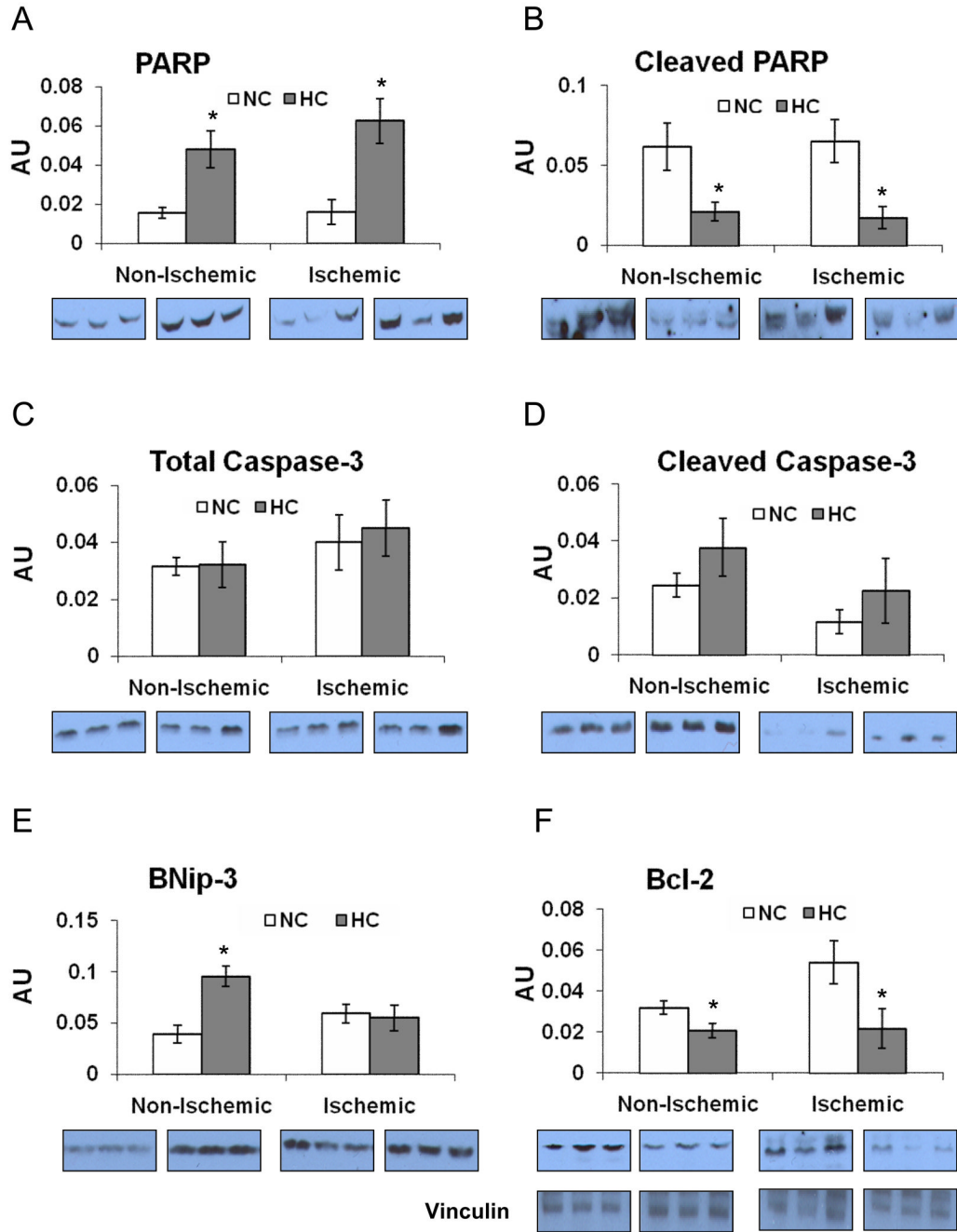


Figure 6. The expression of proteins involved in apoptotic pathway: A) Poly ADP-ribose polymerase (PARP), and B) Cleaved PARP(Asp214), C) Total caspase-3 (p=0.9), D) Cleaved caspase-3 (Asp175) expression was not different between both groups either in the ischemic (p=0.2) or in the non-ischemic (p=0.4) territories, E) BNip-3, F) Bcl2 and vinculin (representative for a loading control) expression. Representative western blots (insets, 3 samples from each group) are shown. Data presented as mean±SEM in arbitrary density units (AU) and compare NC (n=7) and HC (n=7) groups. * p<.05

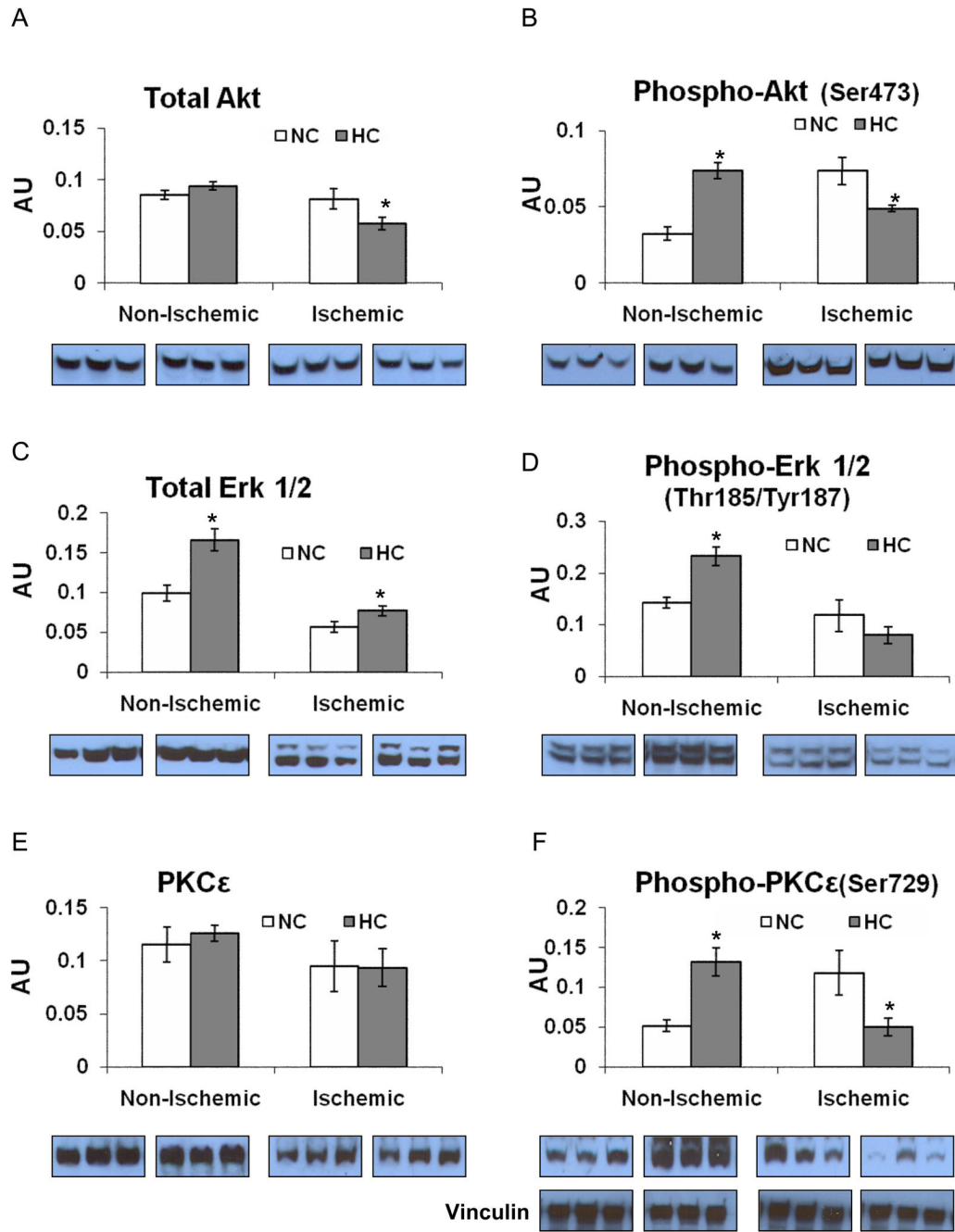


Figure 7. The expression of pro-survival proteins: A) Total Akt, B) Phospho-Akt (Ser473), C) Total Erk 1/2, D) Phospho-Erk 1/2(Thr185/Tyr187), E) Total PKCε, F) Phospho-PKCε and vinculin as a loading control in both the non-ischemic and ischemic territories. Insets show representative western blots for 3 samples from each group. Phospho-PKCε(Ser729) was identified with a phospho-pan-PKC antibody as a band at the same molecular weight as total PKCε. Data presented as mean±SEM in arbitrary density units (AU) and compare NC (n=7) and HC (n=7) groups. * p<.05